Multichromophoric Cyclodextrins. 8. Dynamics of Homo- and Heterotransfer of Excitation Energy in Inclusion Complexes with Fluorescent Dyes

Mario N. Berberan-Santos,*,† Patricia Choppinet,‡,§ Aleksandre Fedorov,† Ludovic Jullien,*,|| and Bernard Valeur*,‡,§

Contribution from the Centro de Química-Física Molecular, Instituto Superior Técnico, 1049-001 Lisboa Codex, Portugal, Laboratoire de Photophysique et Photochimie Supramoléculaires et Macromoléculaires, Ecole Normale Supérieure de Cachan (CNRS UMR 8531), 61 Avenue du Président Wilson, 94235 Cachan Cedex, France, Laboratoire de Chimie Générale, Conservatoire National des Arts et Métiers, 292 rue Saint-Martin, 75003 Paris, France, Département de Chimie, Ecole Normale Supérieure (CNRS UMR 8640), 24 rue Lhomond, 75005 Paris, France

Received March 20, 2000. Revised Manuscript Received October 2, 2000

Abstract: The water-soluble β-cyclodextrin, CD-St, with seven steroidic naphthalene chromophores linked to the primary rim, can form inclusion complexes with a merocyanine dye (DCMOH) and an oxazine dye (Ox725); the stoichiometry is 2:1 (CD-St:dye). This system works as an antenna since the dye is surrounded by 14 chromophores. The efficiency of transfer from the antenna chromophores to the encased dye was found to be close to 100%. The dynamics of this heterotransfer and homotransfer (i.e., energy hopping among the antenna chromophores) was investigated by time-resolved fluorescence intensity and time-resolved fluorescence anisotropy experiments, respectively. The distribution of rate constants for homotransfer was recovered thanks to a previously described Monte Carlo simulation from which an average rate constant was calculated and found to be about 4×10^{11} s^{-1}. This value is about 10 times faster than the rate constant for heterotransfer in the case of Ox725, and about three times faster than in the case of DCMOH. The results are discussed in terms of interchromophoric distances, mutual orientations and Förster radii.

I. Introduction

In previous papers, we have shown the interest of multichromophoric cyclodextrins (i) as models for the study of *excitation energy transport*[1−4] (within a limited number of chromophores) and *antenna effect*[5,6] (i.e., energy transfer from the appended antenna chromophores to an encased acceptor), (ii) as *nanoreactors* for inducing selective photoreactions within the cavity by energy transfer from the antenna chromophores,[7] (iii) as *fluorescent nanosensors* of cationic surfactants or other cationic species.[8]

A major interest of multichromophoric cyclodextrins is to mimic the photosynthetic light-harvesting antennae.[1−6,9] During the past decade, much effort has been indeed focused on the understanding of the first steps of photosynthesis.[10] In this respect, multichromophoric cyclodextrins are good models because the circular arrangement of the chromophores is reminiscent of the light-harvesting complexes of photosynthetic bacteria (LH1 and LH2).[11] Other artificial light-harvesting antennae based on dendrimers,[12] polymers,[13] and arrays of porphyrins[14] or coumarins[15] have also been recently designed.

The aim of the present report is to further investigate the

† Instituto Superior Técnico.
‡ Ecole Normale Supérieure (Cachan).
§ Conservatoire National des Arts et Métiers.
|| Ecole Normale Supérieure (Paris).

(1) Berberan-Santos, M. N.; Canceill, J.; Brochon, J. C.; Jullien, L.; Lehn, J. M.; Pouget, J.; Tauc, P.; Valeur, B. *J. Am. Chem. Soc.* **1992**, *114*, 6427−6436.
(2) Berberan-Santos, M. N.; Pouget, J.; Valeur, B.; Canceill, J.; Jullien, L.; Lehn, J.-M. *J. Phys. Chem.* **1993**, *97*, 11376−11379.
(3) Berberan-Santos, M. N.; Canceill, J.; Gratton, E.; Jullien, L.; Lehn, J.-M.; Peter So, P.; Sutin, J.; Valeur, B. *J. Phys. Chem.* **1996**, *100*, 15−20.
(4) Berberan-Santos, M. N.; Choppinet, P.; Fedorov, A.; Jullien, L.; Valeur B., *J. Am. Chem. Soc.* **1999**, *121*, 2526−2533.
(5) Jullien, L.; Canceill, J.; Valeur, B.; Bardez, E.; Lehn, J.-M. *Angew. Chem., Int. Ed. Engl.* **1994**, *33*, 2438−2439.
(6) Jullien, L.; Canceill, J.; Valeur, B.; Bardez, E.; Lefèvre, J. P.; Lehn, J.-M.; Marchi-Artzner, V.; Pansu, R. *J. Am. Chem. Soc.* **1996**, *118*, 5432−5442.
(7) Wang, P.; Jullien, L.; Valeur, B.; Filhol, J.-S.; Canceill, J.; Lehn, J.-M. *New J. Chem.* **1996**, *20*, 895−907.
(8) Choppinet, P.; Jullien, L.; Valeur, B. *J. Chem. Soc., Perkin. Trans. 2.* **1999**, 249−255.
(9) Gravett, D. M.; J. Guillet, J. *J. Am. Chem. Soc.* **1993**, *115*, 5970−5974.
(10) van Grondelle, R.; Somsen, O. J. G. In *Resonance Energy Transfer*; Andrews, D. L., ed.; Wiley & Sons: 1999; pp 366−398. van Grondelle, R.; Monshouwer, R.; Valkunas, L. *Ber. Bunsen-Ges. Phys. Chem.* **1996**, *100*, 1950−1957. Pullerits, T.; Sundström, V. *Acc. Chem. Res.* **1996**, *29*, 381−389.
(11) (a) McDermott, G.; Prince, S. M.; Freer, A. A.; Hawthornthwaite-Lawless, Papiz, M. Z.; Cogdell, R. J.; Isaacs, N. W. *Nature* **1995**, *374*, 517−521. (b) Hu, X.; Schulten, K. *Phys. Today* **1997** (August), 28−34.
(12) (a) Stewart, G. M.; Fox M. A. *J. Am. Chem. Soc.* **1996**, *118*, 4354−4360. (b) Devadoss, C.; Bharathi, P.; Moore, J. S. *J. Am. Chem. Soc.* **1996**, *118*, 9635−9644. (c) Kopelman, R.; Shortreed, M.; Shi, Z.-Y.: Tan, W.; Xu, Z.; Moore, J. S.; Bar-Haim A.; Klafter, J. *Phys. Rev. Lett.* **1997**, *78*, 1239−1242. (d) Bar-Haim A.; Klafter, J.; Kopelman, R. *J. Am. Chem. Soc.* **1997**, *119*, 6197−6198. (e) Mukamel, S. *Nature* **1997**, *388 (6641)*, 425−427. (f) Jiang, D.-L.; Aida, T. J. *J. Am. Chem. Soc.* **1998**, *120*, 10895. (g) Gilat, S. L.; Adronov, A. Fréchet, J. M. J. *Angew. Chem., Int. Ed.* **1999**, *38*, 1422. (h) Yeow, E. K. L.; Ghiggino, K. P., Reek, J. N. H.; Crossley, M. J.; Bosman, A. W.; Schenning, A. P. H. J.; Meijer, E. W. *J. Phys. Chem.* **2000**, *104*, 2596−2606.
(13) Dupray, L. M.; Devenney, M.; Striplin, D. R.; Meyer, T. J. *J. Am. Chem. Soc.* **1997**, *119*, 10243−10244.
(14) Van Patten, P. G.; Shreve, A. P.; Donohoe, R. J. *J. Phys. Chem.* **1998**, *102*, 4209.
(15) Tyson, D. S.; Castellano, F. N. *Inorg. Chem.* **1999**, *38*, 4382.

10.1021/ja000995l CCC: $19.00 © 2000 American Chemical Society
Published on Web 11/17/2000

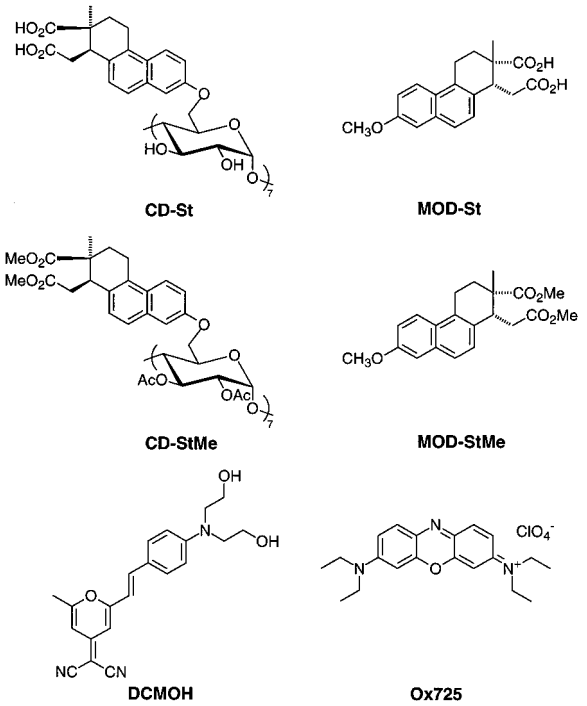

Figure 1. Chemical formulas of CD-St, MOD-St, CD-StMe, MOD-StMe, DCMOH and Ox725.

light-harvesting properties of multichromophoric cyclodextrins, and more precisely, to compare the dynamics of excitation energy transport among the antenna chromophores (homotransfer) with the dynamics of energy transfer from the antenna chromophores to an encased acceptor (heterotransfer). For this investigation, excimer formation between antenna chromophores should be avoided because excimers act as energy traps in the excitation energy hopping process, and energy transfer to an acceptor included in the cavity can occur from both monomer and excimer forms of the antenna chromophores. With this in mind, a new water-soluble β-cyclodextrin CD-St was synthesized; the synthesis together with the photophysical and structural features of its inclusion complexes with a merocyanine dye (DCMOH) and an oxazine dye (Oxazine 725) (see Figure 1) were reported in the preceding paper of this series.[16] The formation of two complexes, CD-St:Dye and $(\text{CD-St})_2$:Dye, was observed and the constants for the following equilibria

$$\text{CD-St} + \text{Dye} = [\text{CD-St:Dye}]$$

$$\text{CD-St} + [\text{CD-St:Dye}] = [(\text{CD-St})_2\text{:Dye}]$$

were found to be 10^4 and 10^7, respectively; therefore, at micromolar concentrations of CD-St and the dyes, the formation of 1:1 complex can be ignored, and only the 2:1 complex (Figure 2) will be considered in the present work. This complex is an outstanding artificial antenna with 14 chromophores surrounding an energy acceptor.

Steady-state and time-resolved fluorescent experiments have been carried out in the presence and in the absence of dye in the cavity. The obtained rate constants for transfer will allow us to compare the dynamics of homotransfer and heterotransfer. In particular, this comparison makes it possible to evaluate such multichromophoric systems for improving the turnover rate of a fluorescent acceptor under given conditions of illumination.

(16) Choppinet, P.; Jullien, L.; Valeur, B. *Chem. Eur. J.* **1999**, *5*, 3666−3678.

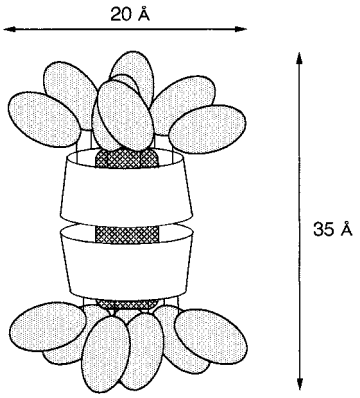

Figure 2. Schematic representation of the $(\text{CD-St})_2$:Dye complex.

II. Results and Discussion

A. Preliminary Discussion on the Mechanisms of Energy Transfer in Multichromophoric Cyclodextrins. Before reporting the results on the new cyclodextrin CD-St, it is worth discussing the possible mechanisms of homotransfer and heterotransfer in free CD-St and its complexes in light of our previous investigations on multichromophoric cyclodextrins.[1−6]

Homotransfer. In CD-St, the chromophores are attached to the primary rim so that the distance between the links of the chromophores to the rim is about 4 Å. The question then arises as to whether the short-range interactions resulting from interchromophore orbital overlap play a significant role or not as compared to Coulombic interactions. It should be first emphasized that, owing to the flexibility of the link between the chromophores and the cyclodextrin rim, a distribution of mutual distances and orientations is expected and that the interchromophoric distance can be significantly larger than 4 Å.

The relative contribution of Coulombic and short-range interactions is an important point to be discussed. The electronic coupling can be written as[17]

$$u = u^{\text{Coul}} + u^{\text{short}}$$

where u^{Coul} is the Coulombic interaction and u^{short} expresses the interactions that depend on the degree of interchromophore orbital overlap. u^{short} is the sum of two terms: (i) u^{exch} defining the quantum mechanical two-electron-exchange interaction; (ii) u^{pen} accounting for interpenetration of the orbitals centered on the two chromophores. Therefore, interpenetration as well as exchange effects are important at close separations, whereas Dexter[18] discussed only the exchange interaction. Interestingly, the u^{pen} term acts to reinforce the u^{Coul} term, while u^{exch} opposes it. Regarding the relative contribution of the Coulombic and short-range interactions, it is of major interest to recall the very interesting results obtained by Scholes and Ghiggino[17] in the case of naphthalene dimers: for instance, at an interchromophoric distance as short as 4 Å, the contribution of short-range interactions to the overall calculated electronic coupling is only 17%. The important consequence is that for allowed transitions the Coulombic interaction is likely to be predominant even at short distances.

One now faces the question as to whether Förster's theory relevant to dipole−dipole interaction[19] is valid in the present

(17) Scholes, G. D.; Ghiggino, K. P. *J. Phys. Chem.* **1994**, *98*, 4580.
(18) Dexter, D. L. *J. Chem. Phys.* **1953**, *21*, 836−850.
(19) (a) Förster, Th. *Ann. Phys. (Leipzig)* **1948**, *2*, 55−75. (b) Förster, Th. *Discuss. Faraday Soc.* **1959**, *27*, 7−17. (c) *Modern Quantum Chemistry*, Part III; Sinanoglu, O., Ed.; Academic Press: New York, 1965; pp 93−137.

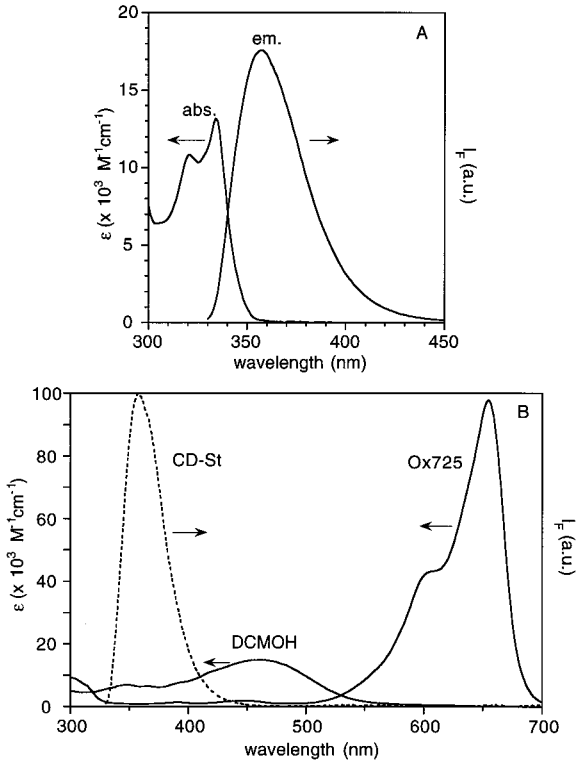

Figure 3. (A) Absorption spectrum and corrected fluorescence spectrum of CD-St. (B) Fluorescence spectrum of CD-St and absorption spectra of DCMOH and Ox725. Solvent: mixture of buffer at pH 10 (I = 0.1 M) and ethanol 95:5 (v/v).

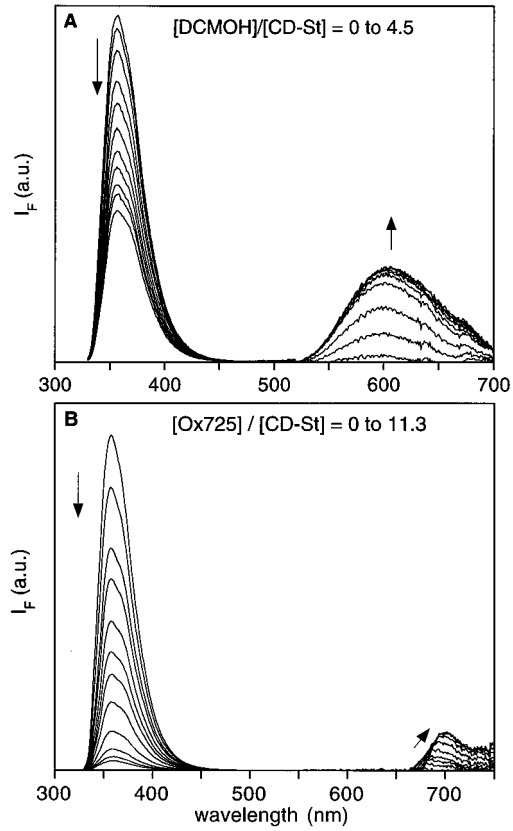

Figure 4. Corrected fluorescence spectra of CD-St/Dye mixtures (λ_{exc} = 320 nm) as a function of the dye concentration. The CD-St concentration is constant during these experiments (A: 9.4 μM with DCMOH; B: 6.8 μM with Ox725). The spectra were corrected for the inner filter effect. Solvent: mixture of buffer at pH 10 (I = 0.1 M) and ethanol 95:5 (v/v).

system. In fact, the point dipole approximation in Förster's theory is questionable in our case because the donor−acceptor separation approaches the size of the chromophores. The Coulombic term must take into account the shape of the molecular charge distribution. This can be achieved by considering the total excitation as a sum of electrostatic interactions between point monopoles located at the atoms of the chromophores,[20] but generally the monopole corrections do not exceed 20%. For instance, despite the small interchromophoric separation between the bacteriochlorophyll a molecules in the LH2 light-harvesting antenna complex of *Rhodobacter sphaeroides*, the monopole corrections were found to be only 20% or less.[21]

All these considerations led us to make the approximation of pure dipole−dipole interaction, that is, very weak coupling, and to use the Förster formula[19b] in the Monte Carlo simulations carried out to estimate the distribution of rate constants for homotransfer.[4] Using the results of these simulations, a good fit to the experimental fluorescence anisotropy decays was obtained for four different multichromophoric cyclodextrins, and the recovered parameters (fundamental anisotropy and nearest-neighbor distance from the anisotropy decay; nearest-neighbor distance from the steady-state anisotropy) for all cyclodextrins were found to be physically reasonable and coherent. In particular, the nearest-neighbor distances fell in the range 5−7 Å in all cases, which is compatible with the nearest-neighbor distances expected from molecular modeling. These observations confirm the validity of the theoretical model based on Förster's theory.

Heterotransfer. In the complexes of CD-St, the distance between the antenna chromophores and an acceptor included into the cavity may be short enough to allow the molecular orbitals of the former to overlap those of latter. The above considerations on electronic coupling between two identical chromophores still apply in the case of two interacting non-identical chromophores, and the conclusions are equally valid. Therefore, the Coulombic interaction is again likely to be predominant.

B. Energy Transfer from the Antenna Chromophores to the Acceptor (Heterotransfer). All experiments were performed at room temperature in an aqueous buffer at pH 10 (ionic strength 0.1 M) containing 5% (v/v) ethanol.

Steady-State Measurements. The absorption and fluorescence spectra of CD-St together with the absorption spectra of the dyes are shown in Figure 3 to visualize the spectral overlap between donor emission spectrum and acceptor absorption spectrum.

Figure 4 displays the evolution of the fluorescence spectrum upon CD-St excitation (λ_{exc} = 320 nm) when increasing the dye concentration at constant CD-St concentration. A progressive quenching of CD-St fluorescence is shown to be accompanied by an increase of dye fluorescence. Moreover, the fluorescence emission arising from the dye exceeds the value expected from direct excitation of the dye. In line with the preceding paper,[16] these experiments confirm: (i) the formation of complexes between CD-St and the dyes; (ii) the process of energy transfer occurring from CD-St to the dye.

The evolution of the fluorescence intensity I_x from CD-St as a function of dye concentration contains information on the stability constant of the complex (β) and on the energy transfer

(20) Chang, J. C. *J. Chem. Phys.* **1977**, *67*, 3901−3909.
(21) Jimenez, R.; Dikshit, S. N.; Bradforth, S. E.; Fleming, G. R. *J. Phys. Chem.* **1996**, *100*, 6825−6834.

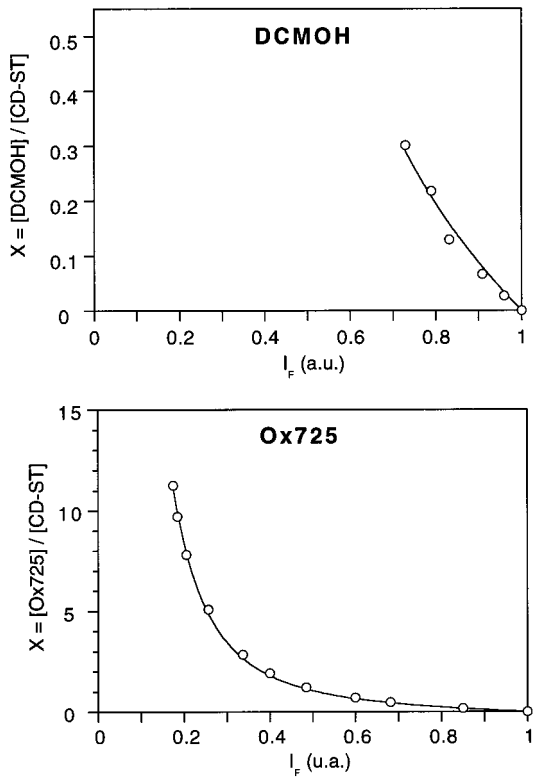

Figure 5. Variations of the ratio $x = [\text{Dye}]_{\text{tot}}/[\text{CD-St}]_{\text{tot}}$ as a function of the fluorescence intensity at 357 nm. The solid lines corresponds to the best fit with eq 1 (see text).

efficiency. In fact, the latter is directly related to the asymptotic value of the fluorescence intensity (corresponding to full complexation).

As explained in the Introduction, a 2:1 complex $[(\text{CD-St})_2\text{:Dye}]$ is solely considered according to the chemical equation:

$$2\text{CD-St} + \text{Dye} = [(\text{CD-St})_2\text{:Dye}]$$

Activities and concentrations were identified in the expression of the corresponding association constant $\beta = [(\text{CD-St})_2\text{:Dye}]/[2\text{CD-St}]^2[\text{Dye}]$ (reference state: solute at infinite dilution) to derive the reported numerical values. Then, the mass conservation conditions, together with the linear dependence of the fluorescence intensity on concentration valid in the dilute regime considered, were used to obtain the following equation:

$$x = \frac{I_x - I_0}{2(I_\infty - I_0)}\left\{\frac{1}{\beta}\left[\frac{1}{[\text{CD-St}]_{\text{tot}}}\left(\frac{I_0 - I_\infty}{I_x - I_\infty}\right)\right]^2 + 1\right\} \qquad (1)$$

where $x = [\text{Dye}]_{\text{tot}}/[\text{CD-St}]_{\text{tot}}$ (the subscript tot refers to the total amount of added solute), and I_0 and I_∞ designate the I_x values of the fluorescence intensity for $x = 0$ and $x \rightarrow \infty$ (full complexation), respectively.

The variations in fluorescence intensity I_x at 357 nm upon addition of DCMOH and Ox725 were corrected for the inner filter effect[16] and then analyzed by using a nonlinear least-squares method (Figure 5).

In the case of Ox 725, the data were first analyzed leaving β and I_∞ as floating parameters. The value found for β was $(2.4 \pm 0.1) \times 10^{10}$, which is in reasonable agreement with the value of 5×10^{10} obtained by a more accurate method described in the preceding paper.[16] The asymptotic value I_∞ was found to be very close to zero within experimental error which led us to the important conclusion that the energy transfer efficiency is close to 1.

The complete set of experimental points were used with Ox725, whereas the DCMOH aggregation[16] precluded analysis of the data when the total DCMOH concentration exceeds 8 μM. Therefore, it turned out to be impossible to get a reliable value of the asymptotic value, and therefore on the energy transfer efficiency. However, this efficiency is expected to be even larger than in the case of Ox725, that is, closer to 1, because the spectral overlap between the emission spectrum of CD-St and the absorption spectrum of the dye is larger for DCMOH than for Ox725 (see Figure 3).

It is easy to show that the transfer efficiency is indeed expected to be close to 1. In the frame of Förster's theory whose validity has been discussed in section A, the transfer efficiency is given by

$$\Phi_{\text{T}} = \frac{1}{1 + \left(\frac{R}{R_0}\right)^6} \qquad (2)$$

where R_0 is the Förster critical radius and R is the donor−acceptor distance. Assuming that no preferential orientation is induced by inclusion of the dye into the cavity, the dynamic average of the orientational factor κ^2, that is, $^2/_3$, can be taken. The values of R_0 are then (34 ± 2) Å for DCMOH and (25 ± 2) Å for Ox725 (see Experimental Section).

By taking reasonable values of R ranging from 5 to 15 Å (see Figure 2), the transfer efficiency is indeed found to be close to 1: in the range 0.993−0.999 for DCMOH and in the range 0.956−0.999 for Ox725.

Time-Resolved Fluorescence Experiments. The fluorescence decay of CD-St alone (excitation at 326 nm and observation at 360 nm) was first recorded in the buffer at pH 10. A small departure from a single exponential was observed: in addition to the major component of 13.1 ns, there was a small contribution (3%) of a shorter component (2.94 ns) to the total intensity (Table 1). The intensity-averaged lifetime (defined as $\langle\tau\rangle = \Sigma\alpha_i\tau_i^2/\Sigma\alpha_i\tau_i$ where α_i and τ_i are the preexponential factors and time constants, respectively) is 12.8 ns.

The fluorescence decays of CD-St were then recorded in the presence of DCMOH at the same excitation and observation wavelengths (Figure 6). The concentrations of CD-St and DCMOH were chosen to be 16.6 μmol.L^{-1} so that the relative fractions of filled and free CD-St were 0.90 and 0.10, respectively. The unquenched fluorescence intensity of the free cyclodextrins is expected to be predominant at long times. A very satisfactory fit of the decay curves was obtained with a sum of three exponentials. No significant improvement of the fit was observed using a sum of four exponentials. To improve the accuracy on the observed short decay time that corresponds to the transfer from the antenna chromophores to DCMOH within the complexes, a narrow channel width was selected (0.955 ps/channel) and two decay times were fixed at the values corresponding to those of the free CD-St (vide supra). Under these conditions, the value of the short decay time is about 40 ps (Table 1). The reconvoluted curve superimposes very well the experimental curve over the whole time range, even in the rise-time part of the exciting pulse (Figure 6A). Comparison with the time evolution of the fluorescence intensity that would have been recorded in the absence of acceptor was made by reconvolution of the double exponential decay with the fixed decay times of the free CD-St (Figure 6B).[22] Since the short

(22) It should be emphasized that the two curves are normalized at long times where the contribution to fluorescence intensity is solely due to the uncomplexed cyclodextrins. One should not forget that a strong quenching of the antenna chromophores is in fact observed.

Table 1. Time Constants Obtained by Analysis of the Time-Resolved Fluorescence of CD-St and Fluorescent Dyes; Excitation Wavelength: 326 nm

acceptor	[CD-St] /μM	[acceptor] /μM	λ_{obs} /nm	channel width/ps	time constants/ns[a] (normalized preexponential factors)	χ_r^{2e}
none	16.6	0	360	51	13.11 (0.88) 2.94 (0.12)	1.28
DCMOH[b]	16.6	16.6	360	0.955	13.11 fixed (0.47) 2.94 fixed (0.29) 0.040 (0.24)	0.95
DCMOH	16.6	16.6	600	0.955	Global analysis with	1.02
	6	6			0.382 fixed, 3.53 fixed	1.06
	60	6			⇒ rise time: 0.042	1.01
DCMOH[c]	60	6	600	0.955	3.53 fixed (1) 0.009 (−0.73) 0.184 (−0.03)	1.03
Ox725[d]	16.6	80.5	360	0.955	13.11 fixed (0.04) 2.94 fixed (0.09) 0.012 (0.73) 0.090 (0.15)	0.90

[a] The accuracy on time constants larger than 100 ps is a few percents. For time constants lower than 100 ps, see text. [b] $[DCMOH]_{free} = 9.0\ \mu M$; $[CD\text{-}St]_{free} = 1.6\ \mu M$; [CD-St:DCMOH] = 0.15 μM; $[(CD\text{-}St)_2{:}DCMOH] = 7.4\ \mu M$. [c] $[DCMOH]_{free} = 0.008\ \mu M$; $[CD\text{-}St]_{free} = 48\ \mu M$; [CD-St:DCMOH] = 0.004 μM; $[(CD\text{-}St)_2{:}DCMOH] = 5.98\ \mu M$. [d] $[Ox725]_{free} = 72.4\ \mu M$; $[CD\text{-}St]_{free} = 1.4\ \mu M$; [CD-St: Ox725] = 1.0 μM; $[(CD\text{-}St)_2{:}Ox725] = 7.1\ \mu M$. [e]

$$\chi_r^2 = \frac{1}{\nu}\sum_{i=1}^{N}\frac{[R(t_i) - R_c(t_i)]^2}{R(t_i)}$$

where $R(t_i)$ is the experimental curve, $R_c(t_i)$ is the calculated one, N is the total number of data points; $\nu = N - p$, where p is the number of fitted parameters.

decay time is of the order of the width of the instrumental response (35−40 ps), careful examination of the accuracy was achieved by calculating the reduced χ-square (defined in Table 1) versus time constant for transfer, all other fit parameters being fixed. The standard deviation is about 10 ps.

The same experiment was carried out with Ox725 upon excitation at 326 nm and observation at 360 nm (Figure 7). In this case, a sum of four exponentials was necessary to obtain a satisfactory fit of the decay curve. As with DCMOH, two of them were fixed at the values corresponding to those of the free CD-St. The decay times relevant to transfer are 12 and 90 ps (Table 1). A standard deviation of 5 ps was evaluated from the variations in reduced χ-square.

To confirm the value of the rate constant for transfer in the DCMOH complex, the acceptor time evolution at 600 nm was measured upon excitation of the antenna chromophores at 326 nm. A rise time should be observed as a result of energy transfer from the antenna chromophores together with the two decay times corresponding to bound and free DCMOH. Three time-resolved experiments were carried out corresponding to three different relative concentrations of CD-St and DCMOH (Table 1). A global analysis (using Globals software) of the three sets of data was performed with a model of three exponentials with two of the time constants were fixed at the values equal to the lifetimes of free DCMOH (0.382 ns) and bound DCMOH (3.53 ns) (these values were determined in a separate experiment upon direct excitation of DCMOH at 575 nm). Then, global analysis yielded a rise time of 42 ps with a standard deviation of about 15 ps, which is in agreement with the decay time previously determined (vide supra).

Unfortunately, it turned out to be impossible to determine the rise time(s) of Ox725 encased in the complex upon excitation of the antenna chromophores because the quantum yield of this dye was too low (even lower than in the buffer).

Discussion. To compare the rates of transfer observed with DCMOH and Ox725, it is convenient to estimate an average value of the time constant for the latter by using the preexponential factors α_i and the time constants τ_i (see Table 1) as follows: $(\alpha_1\tau_1 + \alpha_2\tau_2)/(\alpha_1 + \alpha_2) = 25$ ps.[23] This value is smaller than the time constant for DCMOH (40 ps), which is in contradiction with the spectral overlaps for the two dyes (see Figure 3), and with the resulting Förster critical radii from which it is expected that the energy transfer is faster in complexes with DCMOH than in those with Ox725. Further examination of the time-resolved data will help us to solve this apparent paradox.

By comparing Figures 6B and 7B, it is striking that the effect of energy transfer on the shape of the fluorescence decay of the antenna chromophores is much less pronounced in the case of DCMOH, as revealed by the difference between the experimental curve and the time evolution of the fluorescence intensity that would have been recorded in the absence of acceptor. This is surprising at first sight because the proportions of free and complexed cyclodextrins are the same in the two solutions under study (see Table 1). Moreover, the preexponential factors (Table 1) show that the relative contribution of the time constant for transfer in the case DCMOH (0.24) is much smaller than the sum of the relative contributions of the two time constants for Ox725 (0.88). These considerations led us to conclude that there exist in the case of DCMOH very short time constants (<10 ps) that cannot be determined owing to the time resolution of our instrument. The existence of a very fast initial decay cannot be detected in the very first part of the curve which is affected by the convolution of the δ-pulse response with the instrumental response.

This is confirmed by further analysis of the rise time of the DCMOH fluorescence upon excitation of the antenna chromophores in the presence of an excess of CD-St so that the contribution of direct excitation of free DCMOH molecules is

(23) This expression of the amplitude-averaged time constant must be used in the case of energy transfer. It is not correct to use the intensity-averaged decay time ($\Sigma\alpha_i\tau_i^2/\Sigma\alpha_i\tau_i$) because such an integrated intensity is not relevant to a dynamic process like energy transfer. In fact, the signal measured at a certain time after excitation is proportional to the number of donor molecules still excited at that time and able to transfer their energy to an acceptor molecule; therefore, the amplitude-averaged decay time should be used.

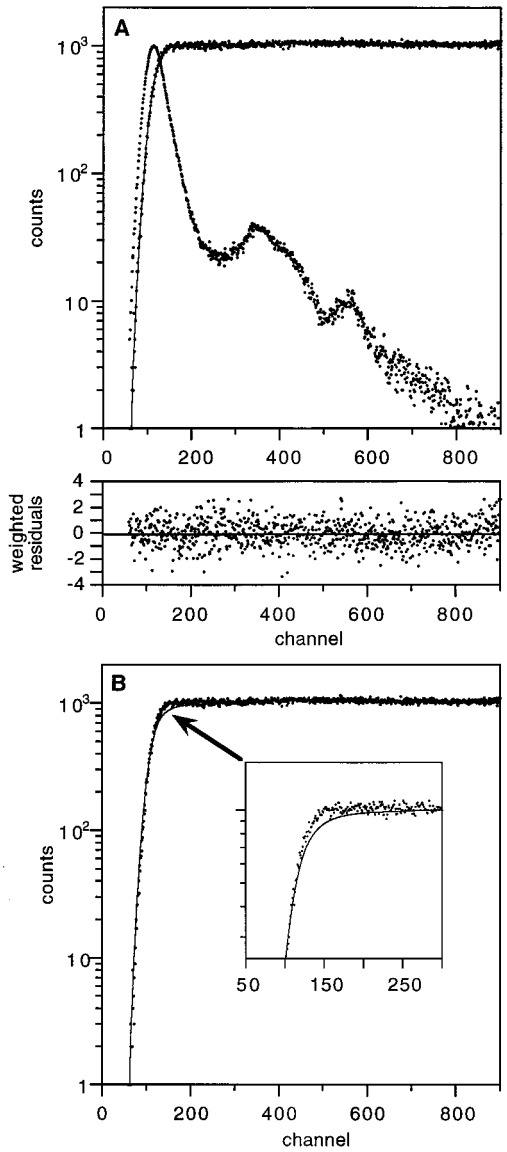

Figure 6. Fluorescence decay of CD-St (16.6 μM) in the presence of DCMOH (16.6 μM). (A) Experimental decay (points) and best fit (solid line) with a sum of three exponentials with two of them fixed at the values corresponding to the empty cyclodextrins (13.11 and 2.94 ns). (B) Reconvoluted curve (solid line) corresponding to only uncomplexed cyclodextrins (with normalization at long time) in order to visualize the effect of energy transfer. The difference between this curve and the experimental decay (points) represents the effect of energy transfer. Excitation wavelength: 320 nm, emission wavelength: 360 nm. Channel width: 0.955 ps.

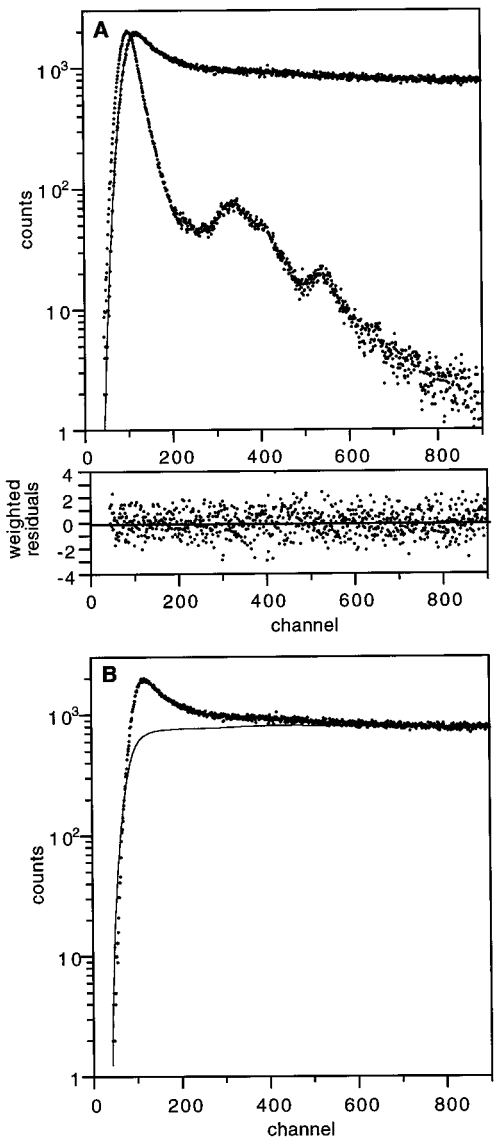

Figure 7. Fluorescence decay of CD-St (16.6 μM) in the presence of Ox725 (80.5 μM). (A) Experimental decay (points) and best fit (solid line) with a sum of four exponentials with two of them fixed at the values corresponding to the empty cyclodextrins (13.11 and 2.94 ns). (B) Reconvoluted curve (solid line) corresponding to only uncomplexed cyclodextrins (with normalization at long time) in order to visualize the effect of energy transfer. The difference between this curve and the experimental decay (points) represents the effect of energy transfer. Excitation wavelength: 326 nm, observation wavelength: 360 nm. Channel width: 0.955 ps.

negligible (Table 1). We tried first a model of a difference of two exponentials. The absolute values of the preexponential factors would be equal if the excited DCMOH molecules appear only by energy transfer from the antenna chromophores. However, direct excitation of a few bound DCMOH is possible at 326 nm. Therefore, the positive preexponential factor is expected to be somewhat larger than the negative one. The decay time was fixed at 3.53 ns (lifetime of bound DCMOH), and the rise time was found to be 37 ps, which is consistent with the value obtained from global analysis). However, the corresponding preexponential factor is -0.14 as compared to the normalized positive preexponential factor of 1, which is not satisfactory at all. Then, we tried a three-exponential model with the decay time still fixed at 3.53 ns and with two floating rise times (Figure 8). The latter ones were found to be 9 and 184 ps (Table 1) with preexponential factors of -0.73 and -0.03, the sum being, as expected, not much smaller than that of the positive preexponential factor normalized to 1. Morever, the chi-square is slightly lower than in the model of a difference of two exponentials and the autocorrelation function of the residuals (not shown) is very satisfactory. It should be emphasized that the rise time of 9 ps has a much larger contribution than the longer one by a factor of more than 20, and considering the width of the instrumental response of our instrument, we cannot indeed exclude the existence of shorter decay times.

The fact that two time constants for energy transfer were determined for Ox725 and DCMOH complexes does not necessarily mean that there are two distinct locations of the dye in the complex. In fact, the analysis described above have shown the difficulty to get reliable values especially when one of the time constants is shorter than the width of the instrumental

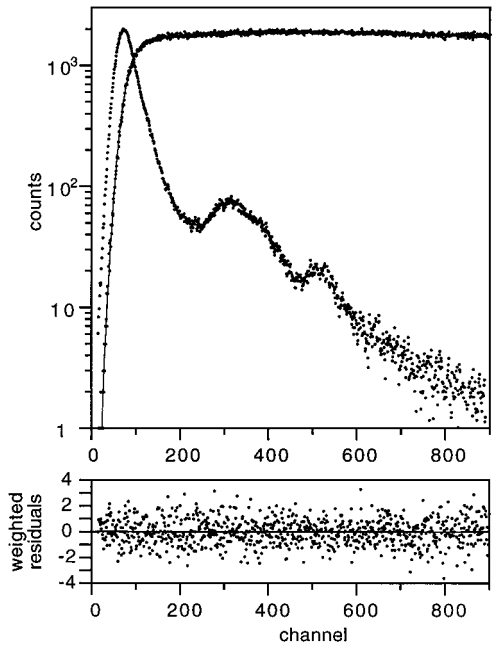

Figure 8. Time evolution of the fluorescence decay of DCMOH (6 μM) in the presence of CD-St (60 μM) (at these concentrations, the amount of free DCMOH is negligible). Experimental decay (points) and best fit (solid line) with a sum of three exponentials with one of them fixed at the value corresponding to the lifetime of bound DCMOH (3.53 ns). Excitation wavelength: 326 nm. Observation wavelength: 600 nm. Channel width: 0.955 ps.

response. Morever, it should be noted that there are various possibilities of relative distances and mutual orientations between the antenna chromophores and a dye molecule included in a 2:1 complex in which the cyclodextrin secondary rims are facing. Therefore, a model based on a sum of one (or two) exponential(s) (fixed) and a distribution of exponentials (expressing a distribution of time constants for transfer) is likely to give an even better curve fitting and would be physically more acceptable. But such a model would be, in practice, difficult to use in data analysis.

From the rate constants, it is, in principle, possible to calculate the average donor−acceptor distance, assuming that the Förster formula can be applied:

$$k = \frac{1}{\tau_0}\left(\frac{R_0}{R}\right)^6 \tag{3}$$

where τ_0 is the excited-state lifetime of the antenna chromophores in the absence of acceptor. However, the above discussion on the rate constants for transfer led us to be very cautions regarding the reliability of such a calculation especially in the case of DCMOH. Moreover, the validity of the point dipole approximation in Förster theory (since the interchromophoric distance is not large with respect to the size of the chromophores) and the value of $^2/_3$ for the orientational factor may be questionable. Nevertheless, assuming random mutual orientations, an order of magnitude can be obtained for the complexes with Ox725. For these complexes, the rate constants for energy transfer (reciprocals of the decay times) are $(1.11 \pm 0.06) \times 10^{10}$ s^{-1} and $(8.3 \pm 0.3) \times 10^{10}$ s^{-1}. Equation 3 leads to values of R equal to 8 and 11 Å which are compatible with the structure of the 2:1 complexes in which the cyclodextrin secondary rims are facing (see Figure 2). But, as outlined above, a conclusion in terms of two different locations of Ox725 cannot be drawn. An average distance of 9−10 Å is preferably to be

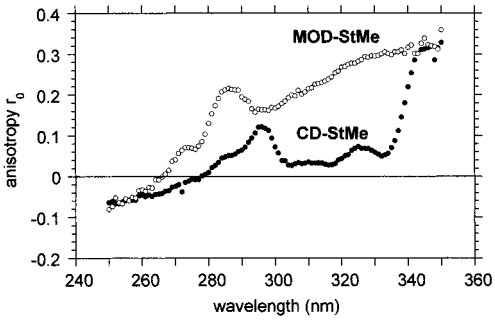

Figure 9. Excitation polarization spectra of MOD-StMe and CD-StMe in a mixture of ethanol−methanol 9:1 (v/v) at 110 K. Observation wavelength: 360 nm.

kept in mind together with an average transfer rate constant of 4×10^{10} s^{-1}.

For DCMOH, the supposed existence of time constants shorter than the instrument response precludes reliable determination of an average distance. Conversely, assuming that the average distance between DCMOH and the antenna chromophores is the same as for Ox725 (i.e., ∼9−10 Å), and taking into account the larger Förster radius (34 Å instead of 25 Å), an average rate constant for heterotransfer is estimated to be about $(1-2) \times 10^{11}$ s^{-1}. The corresponding time constants (5−10 ps) are shorter than the instrument response, as supposed above, and consistent with the predominant short rise time constant of about 9 ps detected in the time evolution of the DCMOH fluorescence.

C. Energy Hopping among the Antenna Chromophores (Homotransfer). For the study of homotransfer, the relevant observable quantity is no longer the fluorescence intensity decay but the emission anisotropy decay. To avoid the depolarization of fluorescence resulting from local motions of the chromophores, the experiments must be done in a rigid glass. An aqueous glass would allow us to study homotransfer and heterotransfer within the complexes under the same conditions. We tried to make such an aqueous glass after adding a large amount of lithium chloride to the buffer at pH 10. Unfortunately, the fluorescence decay of CD-St was very different from a single exponential which renders the use of an average lifetime questionable. Therefore, we decided to make a glass with an ethanol−methanol (9:1) mixture at 110 K. But, since CD-St is poorly soluble in this glass-forming solvent, we used the methylester form of CD-St, denoted CD-StMe. Unfortunately, complexes with DCMOH or Ox725 cannot be formed under these conditions because there is no longer a hydrophobic effect inducing inclusion of the dyes into the cyclodextrin cavity. Consequently, only homotransfer could be studied.

Excitation polarization spectra of MOD-StMe and CD-StMe were recorded under the above conditions (Figure 9). Depolarization resulting from energy transfer is clearly seen, except upon excitation at the red edge of the absorption spectrum (Weber red-edge effect), and to a less extent, upon excitation at the red edge of vibronic bands, as previously reported by us with other multichromophoric cyclodextrins.[2]

Time-resolved anisotropy measurements were also carried out for the above compounds under the same conditions. The excitation and observation wavelengths were 326 and 360 nm, respectively. For MOD-StMe, the emission anisotropy is constant, as expected, and the value, 0.32, is in fair agreement with the steady-state value found to be 0.29. The anisotropy decay of CD-StMe (Figure 10) is very fast: it levels off in less than 100 ps, and the measured long time anisotropy, 0.075, is somewhat higher than the value that would have been expected

from random mutual orientations of the chromophores, that is, $^1/_7$ of the fundamental anisotropy of MOD-StMe at the same excitation wavelength: $0.32/7 = 0.046$. Such a difference could be explained by nonrandom mutual orientations of the chromophores, but in all multichromophoric cyclodextrins previously investigated,[1,4] the chromophores were found to be randomly oriented owing to the flexibility of the link between the chromophores and the cyclodextrin rim. Examination of the excitation polarization spectrum in the 320−330 range (Figure 9) clearly shows that the departure from $r_0/7$ can be assigned to a vibronic red-edge effect.

The time-resolved anisotropy data of CD-StMe were analyzed by using the results of a Monte Carlo simulation previously described by us.[4] It was shown that the anisotropy decay of the heptachromophoric system could be described by a continuous distribution $f(K)$ of rate constants:

$$r(T) = \frac{r_0}{7}\left(1 + 6\int_0^{K_{\max}} f(K)\exp(-KT)dK\right) \qquad (4)$$

$f(K)$ is conveniently expressed with the dimensionless rate constants K defined as $KT = kt$. T is a reduced time, $T = At$, where

$$A = \frac{31}{2\tau_0}\left(\frac{\overline{R_0}}{R}\right)^6 \qquad (5)$$

$\overline{R_0}$ is the value of the Förster radius computed for $\kappa^2 = {}^2/_3$, τ_0 is the excited-state lifetime in the absence of transfer, and R is the nearest-neighbor distance.

It is convenient to define a reduced anisotropy $r_{\mathrm{red}}(T)$ as

$$r_{\mathrm{red}}(T) = \frac{r(T) - r_\infty}{r_0 - r_\infty} = \frac{1}{6}\left(7\frac{r(T)}{r_0} - 1\right) \qquad (6)$$

It decreases from 1 to 0 and its main interest is thus to discard any dependence from r_0 and r_∞. r_0 has indeed nothing to do with energy transfer, and r_∞ is a static parameter that depends on the number of chromophores and their orientations. Hence, the reduced anisotropy wholly characterizes the dynamics of homotransfer.

The reduced anisotropy resulting from the Monte Carlo simulation was shown to be very well-fitted with a sum of hyperbolic terms

$$r_{\mathrm{red}}(T) = \sum_i \frac{G_i}{T + T_i'} \qquad (7)$$

where G_i and T_i' are the best fit parameters of the simulated decay.[24]

In the present case of CD-St, since r_0 and r_∞ are known (0.32 and 0.075, respectively (vide supra)), the reduced anisotropy was calculated and analyzed using the following expression

$$r_{\mathrm{red}}(t) = \sum_i \frac{G_i}{At + T_i'} \qquad (8)$$

where A is the only fitting parameter.

(24) The following values are drawn from Table 1 of ref 4.

G_i	0.415685	1646.422	−2064.425	417.5875
T_i'	0.505293	14.13654	14.41716	15.52145

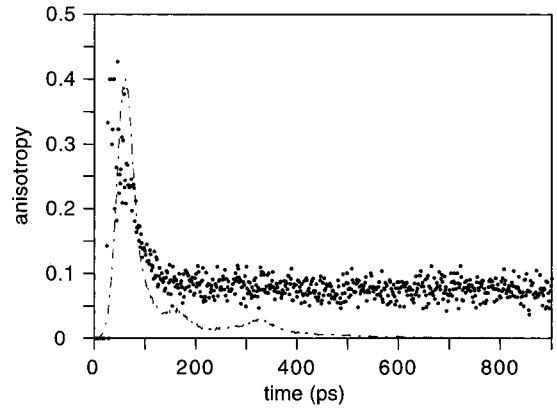

Figure 10. Laser pulse and decay of emission anisotropy of in a mixture of ethanol-methanol 9:1 (v/v) at 110 K. Excitation wavelength: 326 nm, observation wavelength: 360 nm.

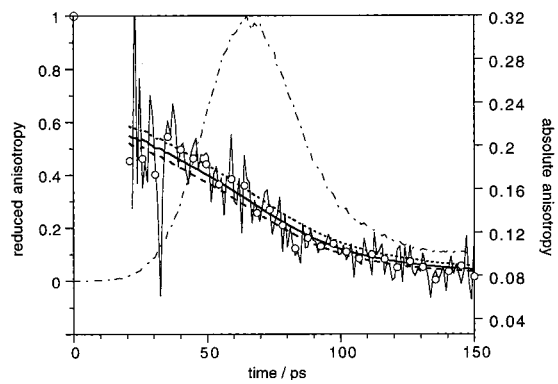

Figure 11. Analysis of the reduced anisotropy decay curve of CD-StMe. The broken lines correspond to $A = 0.20$ ps^{-1} (- - -), 0.25 ps^{-1} (——), 0.30 ps^{-1} (– – –) (see text). Instrument response (– • – • –).

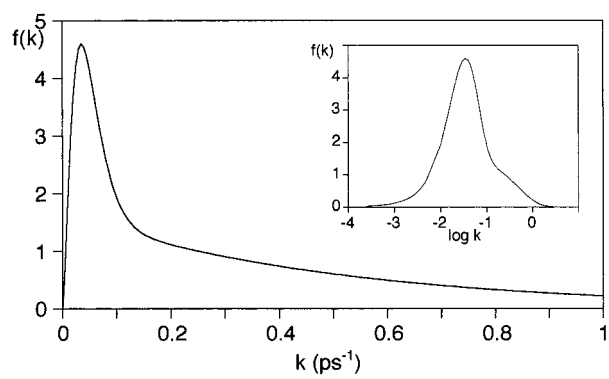

Figure 12. Distribution of rate constants for homotransfer recovered from the analysis of the reduced anisotropy (see text).

Since the anisotropy decay is very fast and occurs during the excitation pulse, analysis was carried out by using eq 11 which takes into account the convolution with the experimental response (see Experimental Section). The experimental reduced anisotropy that was reconstructed with several values of A are shown in Figure 11. A very good agreement is found, *within the pulse duration*, for $A = (0.25 \pm 0.05)$ ps^{-1}. The average rate constant for transfer can then be calculated (see ref 4): $\bar{k} = 1.67A = (0.42 \pm 0.08)$ ps^{-1}. The recovered distribution of rate constants $f(k)$ is shown in Figure 12.

It is of interest to evaluate the highest possible value of the rate constant. In our previous work,[4] it was shown that $K_{\max}$ (in eq 4) is about 10, but a precise value was not determined. Further study allowed us to establish that the configuration for which one of the eigenvalues attains the minimum possible value

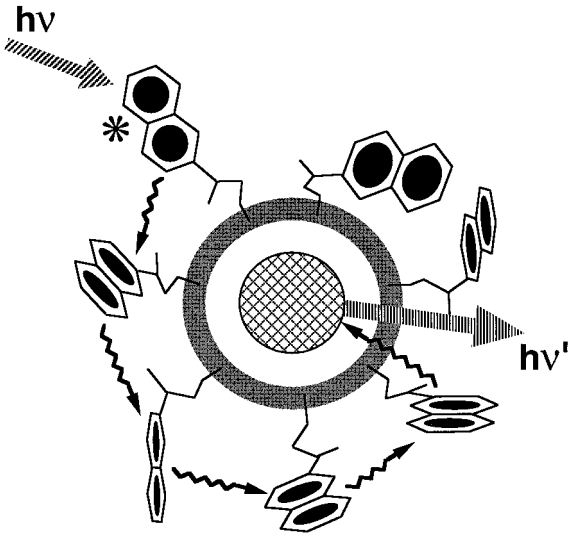

Figure 13. Schematic illustration of excitation energy hopping and trapping.

(maximum in modulus) corresponds to having all the transition dipoles tangential to the circumference defined by the chromophores. This is precisely the case of the photosynthetic units of purple bacteria.[10] In this situation, the orientational factor κ^2 for nearest neighbors is the closest possible to 4, given the constraint of a circular arrangement. For seven chromophores, $\kappa^2 = 3.28$. In this case also, one obtains $K_{max} = 12.54$. In this way, $K_{max}T = K_{max}At = k_{max}t$, hence $k_{max} = 12.54A$, while $\bar{k} = 1.67A$. For $A = 0.25$ ps^{-1}, one obtains $k_{max} = 3.1$ ps^{-1}, which corresponds to a reciprocal time of 320 fs, while the reciprocal of $\bar{k}$ corresponds to 2.4 ps.

From the calculated Förster critical radius (22 Å), the average lifetime (14.7 ns), and the average rate constant ($\bar{k} = 0.42$ ps^{-1}), one obtains $R \cong 7$ Å which is consistent with the value expected from molecular models. It is remarkable that such a nearest-neighbor distance is close to those obtained with other multichromophoric cyclodextrins for which the Förster critical radius was smaller (10 to 15 Å),[4] which resulted in a much slower decay of emission anisotropy (because of the sixth power dependence on R_0/R). These observations further support the validity of the Monte Carlo simulation based on the Förster mechanism for energy transfer.

D. Comparison between Heterotransfer and Homotransfer. The above-described homotransfer experiments were not carried out under the same experimental conditions as heterotransfer. Moreover, CD-StMe was used instead of CD-St. However, the distances between the antenna chromophores in these two cyclodextrins are very similar, and the processes of energy hopping in the two subunits of the 2:1 complexes are likely to be independent. Furthermore, the absorption spectra of CD-StMe and CD-St, their fluorescence quantum yields (0.83 and 0.85, respectively), and their Förster radii for homotransfer (24 and 22 Å, respectively) are very similar. These remarks allowed us to make a comparison between the dynamics of heterotransfer and homotransfer, as schematically represented in Figure 13.

Let us examine first the case of Ox725. The average rate constant for heterotransfer was found to be about 4×10^{10} s^{-1}; this value is to be compared with the average rate constant for homotransfer: 4.2×10^{11} s^{-1}. Consequently, homotransfer appears to be about 10 times faster than heterotransfer. The Förster radius is only slighly shorter for homotransfer (22 Å) than for heterotransfer (25 Å), but the average distance between the antenna chromophores in a 2:1 complex in which the cyclodextrin secondary rims are facing (~6−7 Å) is shorter than the average distance between the dye and the antenna chromophores (~9−10 Å) (vide supra). Because of the inverse sixth power dependence of the rate constant on the interchromophoric distance (eq 3), a 10-fold decrease of the rate constant corresponds to an increase of distance by a factor of only 1.47 (assuming that the Förster radius and the donor lifetime are unchanged). Therefore, the observed factor of 10 is consistent with the average distance between the antenna chromophores and the average distance between the dye and the antenna chromophores.

In the case of DCMOH, the possible existence of time constants shorter than the instrumental time response should be recalled (vide supra). The expected average rate constant (for heterotransfer), $(1-2) \times 10^{11}$ s^{-1}, is three times smaller than the rate for homotransfer. Heterotransfer is, in this case, more competitive with homotransfer because of the larger Förster radius.

In addition to these considerations on distances, effects of relative orientations of the chromophores undergoing transfer should be examined. Under the assumption that the antenna chromophores are randomly oriented, a favorable orientation between an excited chromophore and one of the six others can always be found so that a fast transfer can occur. In contrast, heterotransfer involves an antenna chromophore and the acceptor in a fixed relative orientation. The probability of a favorable mutual orientation is thus lower than in homotransfer; heterotransfer is thus expected to be slower, all other parameters being identical (distances and Förster radius), as observed for Ox725. However, if the Förster radius for homotransfer is smaller than for heterotransfer, the latter can become competitive, as observed for DCMOH.

E. Comparison with Natural Antennae. Natural photosynthetic systems have been optimally selected by evolution for capturing and converting sunlight. In particular, the natural harvesting antenna keeps the reaction center running at an optimal rate (1000 Hz) whereas direct sunlight exposure of the latter would lead to 0.1−10 Hz turnovers at the most.[11b] In relation with this feature, we have been concerned to use the present kinetic results for evaluating the ability of the multichromophoric cyclodextrins to feed the encased fluorescent dyes with excitation energy.

In an antenna−dye system, the antenna effect can be used to decrease the excitation light by a factor $\epsilon_{Antenna}(\lambda_{exc})/\epsilon_{Dye}(\lambda_{exc})$ while maintaining constant the dye emission as long as (i) energy heterotransfer is complete, (ii) the average delay for transferring the excitation from the antenna to the dye is less than the lifetimes of both the dye and the elementary chromophore of the antenna (vide infra). In the [(CD-St)$_2$:dye] complexes, the preceding conditions (i) and (ii) are fulfilled since complete energy transfer from the naphthalene corollas to the encased dyes takes, in average, about 5−25 ps which is much less than the lifetimes of the fluorophores ($\tau \geq 3$ ns). However, the antenna effect is not optimized in multichromophoric cyclodextrins since too few naphthalene chromophores are involved in the process of energy transfer. An order of magnitude of the maximal number of chromophores that could be contained within the antenna while still fulfilling (i) and (ii), can be evaluated as follows. The antenna is assumed to be enlarged while keeping the same homogeneous density of chromophores around the encased dye as in multichromophoric cyclodextrins, that is, keeping an interchromophoric distance of about 1 nm. In addition, we assume that energy hopping proceeds according

to a diffusive mechanism in three dimensions, and each hop corresponds to a distance of $r \approx 1$ nm and takes about $\tau_h = 10$ ps. Then, the maximum distance L between an excited antenna chromophore and the encased dye such that the time required for the excitation energy to reach the dye is less than the fluorophore lifetime can be identified with the spread of excitation energy occurring during time τ. The problem is relevant to excitation transport in restricted media, which is not straightforward,[25] but here only an order of magnitude is searched. By using the classical equations for Brownian motions, one finds $R_{Ant} = [(r^2/\tau_h)\tau]^{0.5} \approx 10$ nm, which is the radius of the largest antenna still meeting the criteria (i) and (ii) mentioned above. Two different situations are now to be examined. The first one aims at finding an appropriate multichromophoric system that could maintain the largest frequency of dye emission, $1/\tau_{Dye}$, but no more than necessary, that is, with an illumination intensity as low as possible. In fact, such a property is highly desirable for applications such as the observation of single fluorescent molecules where multiple excitations often lead to photodestruction.[26] Then, R_{Ant} is limited by the dye lifetime since dye de-excitation must occur before absorption of a new photon conveyed by the antenna. In the present system, $\tau = \tau_{Dye} \approx 3$ ns and $R_{Ant} \approx 40$ nm. In contrast, in a regime of weak illumination, dye de-excitation is not limiting anymore and the magnitude of the antenna effect is controlled by the lifetime of the chromophore antenna. Thus, $\tau = \tau_{Ant} \approx 13$ ns and $R_{Ant} \approx 55$ nm. Both radii are about 20 times larger than that of the present multichromophoric cyclodextrin so that the largest antenna could contain up to 10^4 more elementary chromophores and would then be optimal for feeding the encased dye with excitation energy.

It is now worth examining the efficiency of light collection by the largest antenna as compared to direct excitation of the dye. For the CD-St/DCMOH system, $\epsilon_{CD-St}(340\text{ nm})/\epsilon_{DCMOH}(340\text{ nm}) \approx 5$ and $\epsilon_{DCMOH}(\lambda_{max} = 480\text{ nm})/\epsilon_{CD-St}(340\text{ nm}) \approx 1$. The same frequency of DCMOH emission is thus obtained when (i) directly exciting DCMOH around 480 nm with a light intensity I_0 and (ii) exciting at 340 nm the largest antenna with a light intensity $(2 \times 10^{-5})I_0$. It is interesting to note that the corresponding enhancement of cross section for light collection would then be in the range of the turnover increase that is induced by the natural harvesting antennae which do contain a huge number of participating elementary chromophores.

III. Conclusions

Time-resolved fluorescence experiments allowed us to describe in details the dynamics of excitation energy transfer in 2:1 complexes of a multichromophoric cyclodextrin with fluorescent dyes DCMOH and Ox725. Information on the rate of transfer from the antenna chromophores to the dye was provided by the fluorescence decay of the antenna chromophores in the absence and in the presence of acceptor. Despite the limited time resolution of the instrument, it was possible to conclude that the transfer is faster for DCMOH ($k \approx (1-2) \times 10^{11}$ s^{-1}) than for Ox725 ($k \approx (3-5) \times 10^{10}$ s^{-1}) in accordance with the smaller spectral overlap for the latter, leading to a smaller Förster radius.

Although it turned out to be impossible to study homotransfer under the same experimental conditions as heterotransfer, a comparison of the dynamics of these two processes was attempted. An average transfer rate of $\sim 4 \times 10^{11}$ s^{-1} was determined from the decay of emission anisotropy. Therefore, homotransfer is about 10 times faster than heterotransfer in the case of Ox725, and about three times faster in the case of DCMOH. These differences can be explained in terms of interchromophoric distances, mutual orientations and Förster radii. Consequently, excitation may undergo several hops before being trapped by the acceptor (see Figure 13).

It is worth mentioning that in the bacterial light-harvesting antenna, homotransfer within the B880 ring of LH1 is faster than the transfer from the antenna chromophores to the reaction center.[10] There is thus a strong analogy with the complexes of multichromophoric cyclodextrins investigated in the present work.

IV. Experimental Section

Materials. The syntheses of CD-St, MOD-St, CD-StMe have been already reported.[16]

MOD-StMe has been obtained as the major byproduct during the methylation of bis-dehydro-isomarrianolic acid by diazomethane under the conditions that were reported in ref 16. After recrystallization in MeOH, the melting point was found equal to 109 °C (lit.[27] 107−108 °C). ^{1}H NMR ($CDCl_3$; ref $CHCl_3$ in $CDCl_3$, $\delta = 7.24$ ppm) δ 7.86 (d, $J = 9.2$, 1H, 4′), 7.54 (d, $J = 8.5$, 1H, 7′ or 8′), 7.22 (d, $J = 8.5$, 1H, 7′ or 8′), 7.17 (dd, $J = 2.8$ and 9.2, 1H, 3′), 7.11 (s, 1H, 1′), 3.90 (s, 3H, OCH_3), 3.74 (s, 3H, OCH_3), 3.66 (s, 3H, OCH_3), 3.61 (ddd, $J =$ 1.0, 5 and 6, 1H, 14′), 3.31 (dd, $J = 6.2$ and 18.0, 1H, 11′a), 2.99 (ddd, $J = 7.7$, 11.4 and 18.5, 1H, 11′b), 2.52 (dd, $J = 5.0$ and 15.5, 1H, 15′a), 2.43 (dd, $J = 7.4$ and 15.5, 1H, 15′b), 2.25−2.05 (m, 2H, 12′), 1.23 (s, 3H, 18′); ^{13}C NMR ($CDCl_3$; ref $^{13}CDCl_3$ in $CDCl_3$, $\delta =$ 77.0 ppm) δ_177.4 (16′ or 17′), 172.8 (16′ or 17′), 157.1 (2′), 133.6 (C_{IV}), 132.4 (C_{IV}), 128.8 (C_{IV}), 128.6 (C_H), 127.2 (C_{IV}), 125.6 (C_H), 124.6 (C_H), 118.3 (C_H), 106.5 (C_H), 55.2 (OCH_3), 51.9 (OCH_3), 51.6 (OCH_3), 44.4 (14′), 43.2, 40.9, 24.9, 22.2, 21.7.

4-(Dicyanomethylene)-2-methyl-6-(*p*-(bis(hydroxyethyl)amino)-styryl)-4H-pyran (DCMOH) was synthesized by Dr. J. Bourson according to the general procedure described in ref 28.[28] 3,7-Bis(diethylamino)-phenoxazin-5-ium perchlorate (Ox725) was purchased from Exciton Chemical Co. and was used without further purification.

The Britton−Robinson buffer at pH 10 (ionic strength of 0.1 M) was prepared according to ref 29.[29] Commercially available methanol and ethanol (spectroscopic grade) were used without further purification.

Spectroscopic Measurements: The UV−vis absorption spectra were recorded on a Kontron Uvikon-940 spectrophotometer. Corrected fluorescence spectra were obtained with a SLM 8000 C or a Spex 112 spectrofluorometer. The latter was used to measure steady-state fluorescence anisotropies defined as $r = (I_{\parallel} - I_{\perp})/(I_{\parallel} + 2I_{\perp})$, (where $I_{\parallel}$ and $I_{\perp}$ are the fluorescence intensities observed with vertically polarized excitation light and vertically and horizontally polarized emissions, respectively) by using the *G*-factor method. The low temperature (110 K) measurement methods of the cyclodextrins in an ethanol−methanol (9:1) rigid glass was previously reported.[1]

The overall fluorescence quantum yield of CD-St was previously measured in the buffer at pH 10 and found to be 0.83 ± 0.07.[16] The fluorescence quantum yields of DCMOH and Ox725 in the same buffer were found to be 0.073 and 0.052, respectively.

The Förster critical radius was calculated using the following equation:

$$R_0 = 0.2108[\kappa^2 \Phi_D n^{-4} \int_0^{\infty} I_D(\lambda)\epsilon_A(\lambda)\lambda^4 d\lambda]^{1/6} \qquad (9)$$

with R_0 in Å, where κ^2 is the orientational factor, Φ_D is the quantum yield of fluorescence emission of the donor, n is the average refractive index of the medium in the wavelength range where spectral overlap

(25) *Molecular Dynamics in Restricted Geometries*; Klafter, J., Drake, J. M., Eds.; Wiley & Sons: New York, 1989.

(26) Eggeling, C.; Widengren, J.; Rigler, R.; Seidel, C. A. M. *Anal. Chem.* **1998**, *70*, 2651−2659.

(27) Weidmann, R. *Bull. Soc. Chim. Fr.* **1971**, 912−917.

(28) Bourson, J.; Valeur B. *J. Phys. Chem.* **1989**, *93*, 3871−3876.

(29) Frugoni, C. *Gazz. Chim. Ital.* **1957**, *87*, 403−407.

is significant, $I_D(\lambda)$ is the normalized fluorescence spectrum of the donor, $\epsilon_A(\lambda)$ is the molar absorption coefficient of the acceptor (in $dm^3 \cdot mol^{-1} \cdot cm^{-1}$) and λ is the wavelength in nanometers. As already done,[1,4] the orientation factor was assumed to be equal to the dynamic average, that is, $^2/_3$.

The values of R_0 for CD-St as a donor and DCMOH or Ox725 as acceptors were previously determined and found to be (34 ± 2) Å and (25 ± 2) Å, respectively.[16] The refractive index was chosen to be that of tetrahydrofuran (1.407) since this solvent mimicks the interior of the CD cavity. The standard deviation takes into account the uncertainty on the fluorescence quantum yield and on the refractive index (if n = 1.3 or 1.5 instead of 1.4, R_o is decreased or increased by 1 Å).

For energy hopping among the antenna chromophores (homotransfer), the value of R_0 was determined using the reference chromophore MOD-StMe. The value is (22 ± 2) Å.

Time-Resolved Fluorescence. Time-resolved picosecond fluorescence intensity decays were obtained by the single-photon timing method with laser excitation. The setup consisted of a mode-locked Coherent Innova 400−10 argon-ion laser that synchronously pumped a cavity dumped Coherent 701−2 dye (rhodamine 6G) laser, delivering 3−4 ps pulses (with ∼40 nJ/pulse) at a frequency of 3.4 MHz. Intensity decay measurements were made by alternated collection of impulses and decays with the emission polarizer set at the vertical, horizontal, and magic angle positions. Impulse was recorded slightly away from excitation wavelength with a scattering suspension. For the decays, a cutoff filter was used, effectively removing all excitation light. Detection was always done by passing the emission through a depolarizer and then through a Jobin-Yvon HR320 monochromator with a grating of 100 lines/mm. The *G*-factor of the system is unity, and for the calculation of the anisotropy identical accumulation times were used for both the vertical and the horizontal components, until a total of no less than 20 000 counts at the maximum channel was obtained for the vertical component. A time scale of 18.4 ps/channel was used. The detector employed was a Hamamatsu 2809U-01 microchannel plate photomultiplier. The instrument response function had an effective fwhm of 40 ps.

Squared 5 × 5 mm cuvettes were used in order to reduce timing errors due to the length of the optical path in the cuvette.

Fluorescence intensity decay curves were analyzed by a nonlinear least-squares method using Globals software (Globals Unlimited, University of Illinois at Urbana-Champaign, Laboratory for Fluorescence Dynamics).

Time-resolved anisotropy data were analyzed by using the following equation[30] giving the experimental anisotropy

$$r_{exp}(t) = \frac{E(t) \otimes [r(t)I(t)]}{E(t) \otimes I(t)} \tag{10}$$

where ⊗ denotes the convolution product, $r(t)$ is the δ-pulse response of the anisotropy decay, $I(t)$ is the δ-pulse response of the fluorescence intensity decay, and $E(t)$ is the response function of the instrument. For an anisotropy decay much faster than the intensity decay, which is the case of the present work, the latter equation becomes

$$r_{exp}(t) = \frac{E(t) \otimes r(t)}{E(t) \otimes 1} \tag{11}$$

Acknowledgment. Travel grants to MNBS, PC, and BV from ICCTI (Portugal)-CNRS (France) joint program are acknowledged. AF was supported through a PRAXIS XXI Grant (FCT, Portugal).

JA000995L

(30) Berberan-Santos, M. N. *J. Lumin.* **1991**, *50*, 83−87.